Heat Mass Transfer (2012) 48:789–798
DOI 10.1007/s00231-011-0933-2

ORIGINAL

Simple model for predicting microchannel heat sink performance and optimization

Tsung-Hsun Tsai · Reiyu Chein

Received: 18 January 2011 / Accepted: 28 October 2011 / Published online: 10 November 2011
© Springer-Verlag 2011

Abstract A simple model was established to predict microchannel heat sink performance based on energy balance. Both hydrodynamically and thermally developed effects were included. Comparisons with the experimental data show that this model provides satisfactory thermal resistance prediction. The model is further extended to carry out geometric optimization on the microchannel heat sink. The results from the simple model are in good agreement as compared with those obtained from three-dimensional simulations.

List of symbols

Bi	Biot number
C_i	Coefficients used in evaluating the Nusselt number, i = 1, 2, 3, 4
C_p	Fluid specific heat, J kg^{-1} K^{-1}
D_h	Channel hydraulic diameter, m
fRe	Poiseuille number
H	Microchannel heat sink depth, m
H	Heat transfer coefficient, W m^{-2} K^{-1}
H_b	Microchannel heat sink base plate thickness, m
H_{ch}	Microchannel depth, m
K	Hagenbach's factor
k_f	Fluid thermal conductivity, W m^{-1} K^{-1}
k_s	Solid wall thermal conductivity, W m^{-1} K^{-1}
L	Microchannel heat sink length, m
$\dot{m}$	Mass flow rate, kg s^{-1}
N	Number of microchannels
Nu	Thermally developing Nusselt number for four-sided heating channel
Nu_3	Thermally developing Nusselt number for three-sided heating channel
$Nu_{\infty,3}$	Thermally developed Nusselt number in three-sided heating channel
$Nu_{\infty,4}$	Thermally developed Nusselt number in four-sided heating channel
$\bar{P}$	Pumping power, W
Pr	Prandtl number
q''	Heat flux, W m^{-2}
Re	Reynolds number
R_{th}	Thermal resistance of microchannel heat sink, °C m^2 W^{-1} or °C W^{-1}
T_b	Microchannel heat sink base plate temperature, K
T_f	Fluid temperature, K
T_s	Solid temperature, K
u_m	Mean fluid velocity, m s^{-1}
$\dot{V}$	Volumetric flow rate, m^3 s^{-1}
x^*	Dimensionless location along the flow direction
x^*_{th}	Dimensionless thermal entrance length
W	Microchannel heat sink width, m
W_{ch}	Microchannel width, m
W_f	Wall thickness between microchannels, m

Greek symbols

α	Channel aspect ratio
β	Ratio of the channel width to channel pitch
Δp	Pressure drop, Pa
μ	Fluid viscosity, Pa s
ρ	Fluid density, kg m^{-3}

T.-H. Tsai
Department of Mechanical Engineering,
WuFeng University, Chia-yi 621, Taiwan

R. Chein (✉)
Department of Mechanical Engineering,
National Chung Hsing University,
250 Kuo-Kuang Rd., Taichung City 402, Taiwan
e-mail: rychein@dragon.nchu.edu.tw

1 Introduction

As electronic equipment becomes smaller and more advanced, higher circuit integration per unit area is required, which produces a rapid increase in heat generated from electronic devices. As a consequence, the working temperature of electronic components may exceed the desired temperature level, which increases the circuit failure rate of the equipment in the absence of sufficient heat removal. Therefore, advanced electronic equipment with small size and high heat generation requires efficient and compact cooling devices to provide reliable system operation. In the past two decades, many cooling technologies have been pursued to meet the high heat dissipation rate requirements and maintain low junction temperature. Among these efforts, the microchannel heat sink (MCHS) has received much attention because of its ability to produce high heat transfer coefficient through its small size, volume per heat load and coolant requirements. Recent progress in the development of microchannel heat sinks is provided by Kandlikar and Grande [1].

A microchannel heat sink typically contains a large number of parallel microchannels with a hydraulic diameter ranging from 10 to 1,000 μm. Coolant is forced to pass through these channels to carry the heat away from a hot surface. The concept of MCHS was first proposed for electronic cooling by Tuckerman and Pease [2]. Since then, MCHS performance using different substrate materials and channel dimensions have been studied extensively in the past two decades. These studies can be categorized into theoretical [3–6], numerical [7–17], and experimental approaches [18–21]. In the theoretical approach, the main objective is to develop design schemes that can be used to optimize microchannel heat sink performance. Most studies in this approach employed the classical fin theory, which models the solid walls separating microchannels as thin fins. The heat transfer process is simplified as one-dimensional, constant convection heat transfer coefficient and uniform fluid temperature. However, the nature of the heat transfer process in a microchannel heat sink is conjugated heat conduction in the solid wall and convection to the cooling fluid. The simplifications used in the theoretical approach usually under- or over predict the microchannel heat sink performance.

Although experimental studies have been carried out extensively in the past, it is often difficult to employ conventional measurement techniques with microchannel heat sinks to extract data that are important to characterizing the fluid flow and heat transfer such as local fluid and wall temperature distributions. For this reason, numerical simulation becomes a necessary tool that offers more quantitative insight into the transport process in the MCHS. In the numerical simulation, conventional equations governing the fluid flow and heat transfer are assumed to be valid in the micro-scale dimension. The conjugate heat transfer process between the fluid and solid wall is included. Fedorov and Viskanta [7] numerically analyzed three-dimensional conjugate heat transfer in a MCHS without the hydrodynamic and thermal fully developed flow assumptions. They obtained very complicated heat transfer pattern characterized using a nearly uniform microchannel wall temperature and the negative local heat transfer at the channel corners. Li et al. [8] presented a detailed numerical study of a forced convection heat transfer occurring in a silicon-based MCHS using a simplified three-dimensional conjugated heat transfer model. Detailed influences of the channel geometric dimensions and thermophysical fluid properties of the fluid on the heat transfer characteristics were examined. They indicated that the thermophysical properties of the fluid can significantly influence both the flow and heat transfer in a MCHS. Extending this study, Li and Peterson [9] employed the numerical simulation to optimize the MCHS geometry under constant pumping power condition. They found that both the physical geometry of the microchannel and the thermophysical properties of the substrate are important parameters in the design and optimization of the MCHS. Qu and Mudawar [10, 11] investigated the pressure drop and heat transfer in a single-phase microchannel heat sink both numerically and experimentally. In their numerical simulation, the heat transfer characteristics were obtained by solving the conjugate heat transfer problem involving simultaneous determination of the temperature field in both solid and fluid regions. They compared the numerical results with the experimentally measured data and showed good agreement in pressure drop across the microchannel heat sink and local fluid and wall temperature variations. Liu et al. [12] numerically studied the heat transfer and pressure drop in fractal microchannel heat sink for electronic chip cooling. For electroosmotically driven water flow, Husain and Kim [13] numerically investigated thermal transport characteristics of microchannel heat sink with wavy wall.

In the study of Lee et al. [14], experiments were conducted to explore the validity of classical correlations based on conventional sized channels for predicting the thermal behavior in single-phase flow through rectangular microchannels. A numerical simulation was also carried out and the results were compared with the experimental data. They pointed out that both fluid flow and heat transfer are in developing regime and cannot be neglected in the analysis. Recently, Xia et al. [15] carried the numerical simulation to examine the effect of geometric parameters on water flow and heat transfer characteristics in microchannel heat sink with triangular reentrant cavities. By using the thermal enhancement factor performance maps, they pointed out that the optimal geometric parameters can

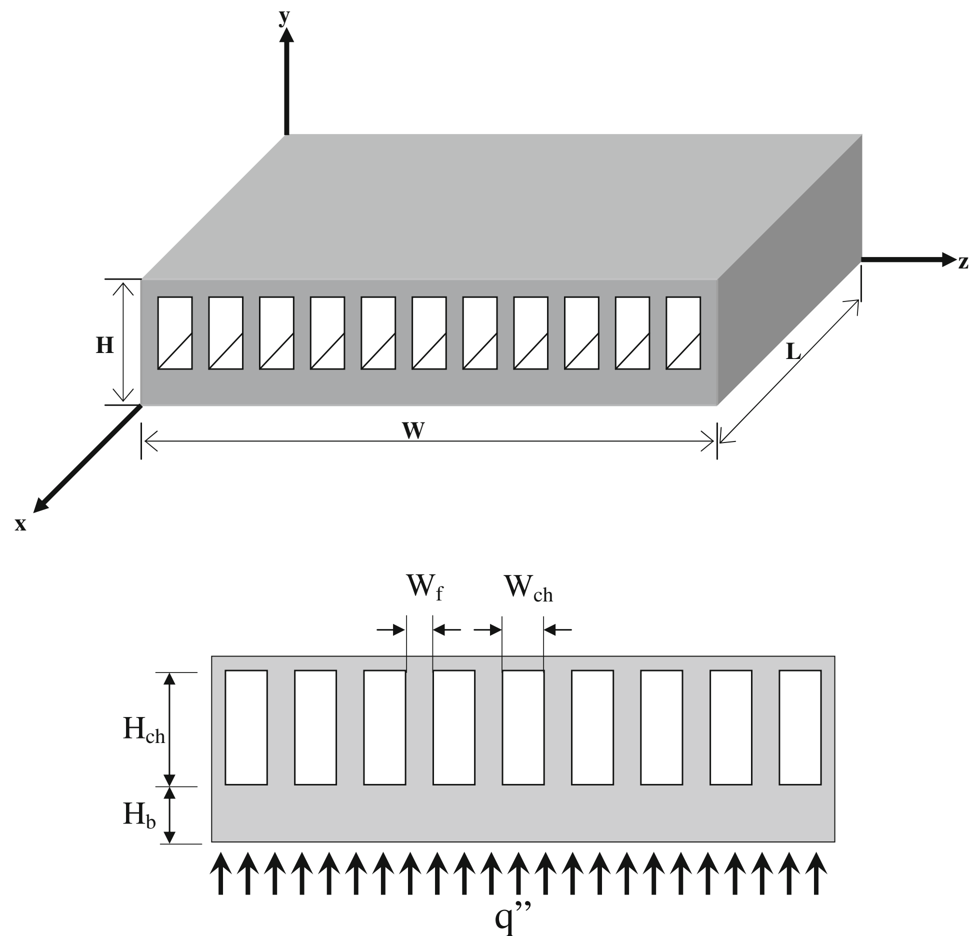

Fig. 1 The schematic and overall dimensions of the MCHS (the drawing is not to scale)

be obtained in principle. In addition to MCHS applications, fundamental understandings regarding the fluid flow and heat transfer characteristics in microchannel were also reported by several studies [16, 17].

Although three-dimensional conjugate heat transfer analyses of MCHS have been shown to provide satisfactory results as compared with the experimental measurements, they are computationally expensive, case-specific and cannot be generalized to a wide range of microchannel configurations. Similarly, experimental approach is also time-consuming and involves experimental uncertainties. The purpose of this study is to formulate a simple model that capable of predicting the MCHS performance without time-consuming three dimensional computations. This model is verified by the experimental data and three-dimensional numerical simulation results reported in the literature.

2 Analytical model

In this study, the schematic of the MCHS under consideration is shown in Fig. 1 having the width of W, length of L and height of H. The microchannel in the heat sink has width and depth of W_{ch} and H_{ch}, respectively. The channels are separated by walls having thickness of W_f. These walls are usually referred to as fins in the study using fin theory. The MCHS base plate thickness H_b is measured from the channel bottom wall to the surface where electronic chip is attached (base plate). The MCHS shown in Fig. 1 can be fabricated using etching or micro-machining technique, depending on the material used. After the fabrication of microchannels, a plate with low thermal conductivity such as glass is bonded on top of the microchannels to form the fluid flow passage. It is assumed that the chip is completely attached to the MCHS base plate and generates a uniform heat flux q''. Coolant with temperature $T_{f,in}$ is forced to flow through the channels to carry the heat away from the chip. The fluid flow is in the x direction.

Since all the channels are geometrically identical and receive the same flow rate and heat flux, the analysis can be restricted to only one channel. The end effect is ignored since the heat transfer from the side walls of the heat sink only affect a few channels in each side of the heat sink. As shown in Fig. 2a, heat spreads in the solid through conduction and enters the fluid flow through convection from

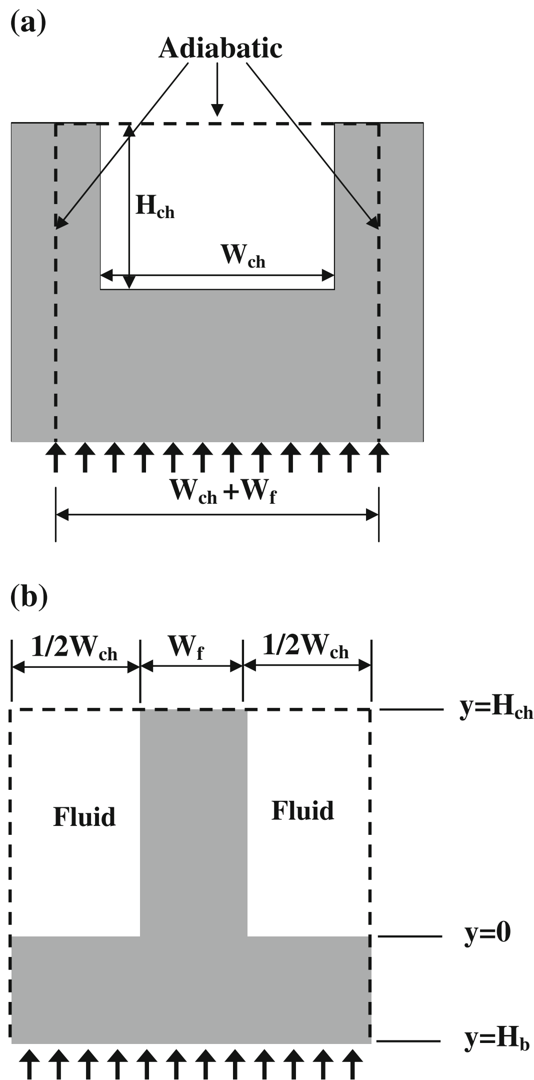

Fig. 2 **a** Unit cell of micro-channel heat sink. **b** Unit cell for fin theory

the inner walls of the channel. In general, this is a three-dimensional conjugate heat transfer problem. However, if the heat sink is fabricated using high thermal conductivity material such as silicon or copper, it can be assumed that the temperature of the inner wall of the channel is uniform at each cross section in the flow direction. Under these conditions, the problem can then be considered as a classical conduction problem in a fin as shown in Fig. 2b. The goal of the analysis is to predict the heat sink base temperature which is the temperature at the base plate of the heat sink.

According to the fin theory, the variation of temperature along the fin at a location x is governed by,

$$\frac{\partial^2 T_s}{\partial y^2} - \frac{2h(x)}{k_s W_f}[T_s - T_f(x)] = 0 \quad (1)$$

where $T_s(x, y)$ is the averaged fin temperature over the fin width, $h(x)$ is the local interfacial heat transfer coefficient, k_s is the solid wall thermal conductivity, and $T_f(x)$ is the fluid temperature averaged over the channel cross section and can be regarded as the bulk fluid temperature. Since the heat fluxes at y = 0 and y = H_b are the same, the boundary conditions for Eq. 1 are,

$$-k_s \frac{\partial T_s}{\partial y}\bigg|_{y=0} = q'' \text{ and } -k_s \frac{\partial T_s}{\partial y}\bigg|_{y=H_{ch}} = 0 \quad (2)$$

The solution of Eq. 1 is,

$$T_s(x,y) = T_f(x) + \frac{q'' W_f}{k_s\sqrt{2Bi}} \frac{\cosh\left[\sqrt{2Bi}(H_{ch} - y)/W_f\right]}{\sinh\left(\sqrt{2Bi}H_{ch}/W_f\right)} \quad (3)$$

where $Bi = h(x)W_f/k_s$ is the Biot number. Using Eq. 3, the averaged fin temperature over the fin length can be obtained as,

$$T_s(x) = T_f(x) + \frac{q'' W_f}{2H_{ch}h(x)} \quad (4)$$

The averaged fin temperature can be regarded as the temperature of the channel inner wall due to high thermal conductivity of the heat sink material. To complete the solution, the bulk fluid temperature along the flow direction needs to be solved. For a given location x in the flow direction, energy balance for the fluid flow can be written as,

$$\dot{m}C_p \frac{dT_f}{dx} = q''(W_f + W_{ch}) \quad (5)$$

Integrating from the inlet of the channel, $T_f(x)$ is obtained as,

$$T_f(x) = T_{f,in} + \frac{q''(W_f + W_{ch})}{\dot{m}C_p} x \quad (6)$$

In Eqs. 5 and 6, C_p is the fluid specific heat, $\dot{m}$ is the mass flow rate in the channel defined as,

$$\dot{m} = \rho W_{ch} H_{ch} u_m \quad (7)$$

where u_m is the mean fluid velocity, ρ is the fluid density. Using Eq. 4, the heat sink base temperature can be obtained from the one-dimensional conduction equation,

$$T_b(x) = T_s(x) + \frac{q'' H_b}{k_s} \quad (8)$$

Since the above-built simple model starts from the channel inlet, the entrance effects for both the fluid flow and temperature distributions can be taken into account. To carry out the calculations using Eqs. 4 and 8, analytical expressions for the interfacial heat transfer coefficients in thermally developing and developed regions are needed. In the thermally developing region, a recently developed heat

transfer coefficient and thermal entrance length correlations as function of channel aspect derived by Lee and Garimella [22] are employed,

$$Nu(x) = \frac{h(x)D_h}{k_f} = \frac{1}{C_1(x^*)^{C_2} + C_3} + C_4 \quad \text{for } 1 \le \alpha \le 10 \text{ and } x^* < x^*_{th} \tag{9}$$

where k_f is the fluid thermal conductivity, D_h is the channel hydraulic diameter, α is the channel aspect ratio, x^* is the dimensionless location along the flow direction, and x^*_{th} is the dimensionless thermal entrance length. These parameters are defined as follows,

$$D_h = \frac{4W_{ch}H_{ch}}{2(W_{ch} + H_{ch})} \tag{10}$$

$$\alpha = H_{ch}/W_{ch} \tag{11}$$

$$x^*_{th} = -1.275 \times 10^{-6}\alpha^6 + 4.709 \times 10^{-5}\alpha^5 - 6.902 \times 10^{-4}\alpha^4 + 5.014 \times 10^{-3}\alpha^3 - 1.769 \times 10^{-2}\alpha^2 + 1.845 \times 10^{-2}\alpha + 5.691 \times 10^{-2} \tag{12}$$

$$x^* = x/(\mathrm{Re}\,\mathrm{Pr}\,D_h) \tag{13}$$

In Eq. 13, Reynolds number Re and Prandtl number Pr are defined as follows,

$$\mathrm{Re} = \rho u_m D_h/\mu \tag{14}$$

$$\mathrm{Pr} = C_p\mu/k_f \tag{15}$$

where μ is the fluid viscosity. The constants C_1, C_2, C_3 and C_4 in Eq. 9 are function of aspect ratio given as,

$$C_1 = -3.122 \times 10^{-3}\alpha^3 + 2.435 \times 10^{-2}\alpha^2 + 2.143 \times 10^{-1}\alpha + 7.325 \tag{16a}$$

$$C_2 = 0.6412 \tag{16b}$$

$$C_3 = 1.589 \times 10^{-4}\alpha^2 - 2.603 \times 10^{-3}\alpha + 2.444 \times 10^{-2} \tag{16c}$$

$$C_4 = 7.148 - 13.28/\alpha + 15.15/\alpha^2 - 5.936/\alpha^3 \tag{16d}$$

Note that Eq. 9 is developed subject to constant heat flux applied around the four sides of the channel. To apply Eq. 9 in the MCHS application in which three-sided heating is involved, correction should be made. As proposed by Phillips [23], the correction of heat transfer coefficient from four-sided heating to three-sided heating can be achieved using the following formula,

$$Nu_3(x) = Nu(x)\frac{Nu_{\infty,3}}{Nu_{\infty,4}} \tag{17}$$

where $Nu_{\infty,3}$ and $Nu_{\infty,4}$ are the heat transfer coefficient correlations in thermally fully developed regions for three- and four-sided heating in laminar rectangular channel flows, respectively. As given by Shah and London [24], $Nu_{\infty,3}$ and $Nu_{\infty,4}$ can be expressed as,

$$Nu_{\infty,3} = 8.235(1 - 1.883/\alpha + 3.767/\alpha^2 - 5.814/\alpha^3 + 5.361/\alpha^4 - 2.0/\alpha^5) \tag{18}$$

$$Nu_{\infty,4} = 8.235(1 - 2.0421/\alpha + 3.0853/\alpha^2 - 2.4765/\alpha^3 + 1.0578/\alpha^4 - 0.1861/\alpha^5) \tag{19}$$

For $x^* > x^*_{th}$, Eq. 18 is employed to evaluate the heat transfer coefficient in the thermally fully developed region.

Using the computed base temperature, the thermal resistance of the heat sink may be calculated. The thermal heat sink resistance is defined as [11, 25],

$$R_{th} = \frac{T_{b,out} - T_{fin}}{q''} \tag{20}$$

where $T_{b,out}$ is the base temperature at the MCHS outlet. Besides the thermal resistance, the pressure drop across the heat sink is another important parameter in heat sink design since it relates to the pumping power required to drive the fluid through the heat sink. In the present study, the formula given by Kandlikar et al. [26] was adopted to predict the pressure drop in which the hydrodynamically developing region effect is included,

$$\Delta p = \frac{2(f\mathrm{Re})\mu \mathrm{u_m L}}{D_h^2} + K(\infty)\frac{\rho u_m^2}{2} \tag{21}$$

where $f\mathrm{Re}$ is the Poiseuille number and $K(\infty)$ is Hagenbach's factor. For laminar flow in rectangular channel, $f\mathrm{Re}$ and $K(\infty)$ are given as [26],

$$f\mathrm{Re} = 24(1 - 1.3553/\alpha + 1.9467/\alpha^2 - 1.7012/\alpha^3 + 0.9564/\alpha^4 - 0.2537/\alpha^5) \tag{22}$$

$$K(\infty) = 0.6796 + 1.2197/\alpha + 3.3089/\alpha^2 - 9.5921/\alpha^3 + 8.9089/\alpha^4 - 2.9959/\alpha^5). \tag{23}$$

3 Results and discussion

3.1 Comparison with existing experimental and numerical results

The predicted results using the simple model developed in this study were compared with the experimental and numerical studies available in the literature. The thermophysical properties of the solid and fluid used in the calculation are listed in Table 1. We first compared the predicted results from the simple model with experimental and numerical results reported by Qu and Mudawar [11]. In

Table 1 Thermophysical properties of heat sink material and working fluid used in the simple model calculation [27]

Material	Density (kg m^{-3})	Thermal conductivity (W m^{-1} K)	Viscosity (Pa s)	Specific heat (J kg^{-1} K)
Water	1,000	0.6	0.00086	4,178
Silicon	2,330	148		712
Copper	8,933	401		385

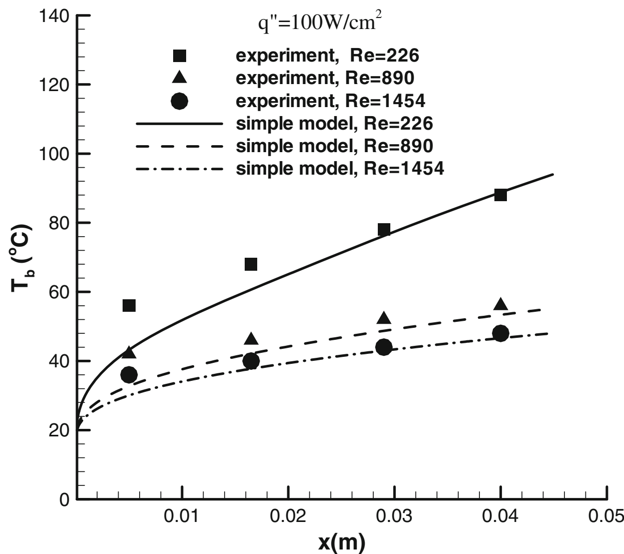

Fig. 3 Comparison of solid temperature distribution along the microchannel predicted by the simple model with experimentally measured data by Qu and Mudawar [11]. q″ = 100 W cm^{-2}

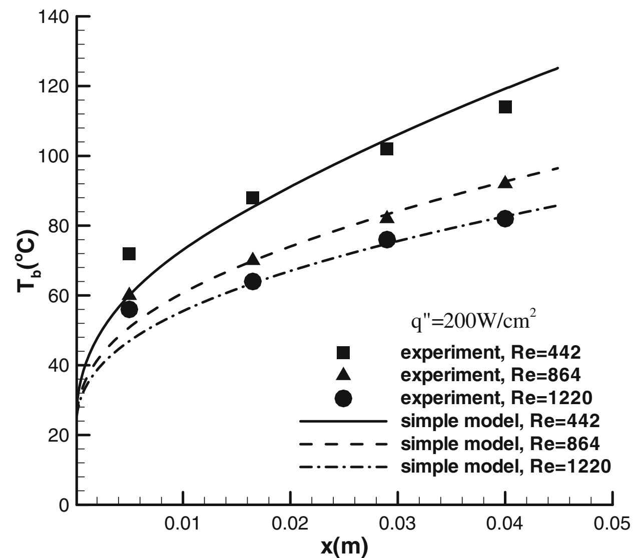

Fig. 4 Comparison of solid temperature distribution along the microchannel predicted by the simple model with experimentally measured data by Qu and Mudawar [11]. q″ = 200 W cm^{-2}

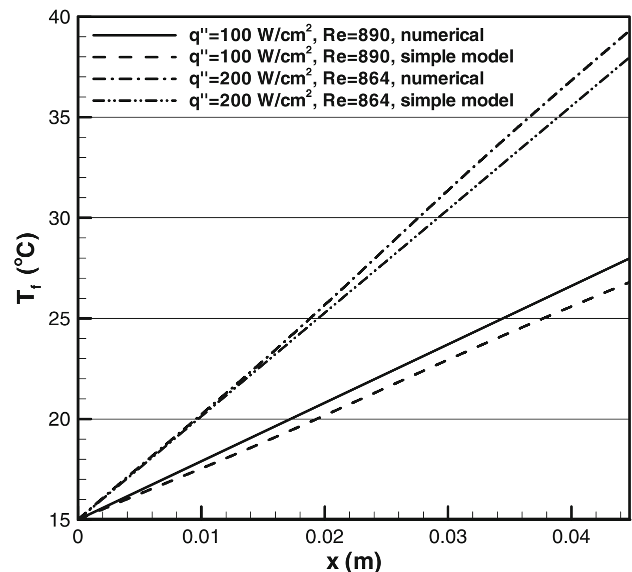

Fig. 5 Comparison of fluid temperature distribution along the microchannel predicted by the simple model with numerically simulated results of Qu and Mudawar [11]

the study of Qu and Mudawar [11], performance of a copper MCHS was investigated under various flow rates and heat fluxes. The heat sink contains parallel microchannels with the dimensions of $W_{ch} = 231$ µm, $H_{ch} = 713$ µm, $W_f = 236$ µm, $H_b = 2462$ µm and L = 44.764 mm. The inlet fluid temperature is $T_{f,in} = 15$°C. Using these dimensions and inlet fluid temperature, the measured and predicted base temperature distributions along the channel length are compared and shown in Figs. 3 and 4 for various heating fluxes and Reynolds numbers. As shown in Figs. 3 and 4, the agreement is good, especially at the channel downstream. Since the entrance effect is a three-dimensional phenomenon, larger discrepancy between the base temperatures predicted by the simple model and experimental data is found at the entrance zone of the channel. As the flow approaching fully hydrodynamic and thermal developed conditions at the channel downstream, the error is found to reduce. In the study of Qu and Mudawar [11], experimental data of the fluid bulk temperature distribution along the channel did not reported because of difficulty associated with the measurement. Instead, they reported the numerically simulated fluid bulk temperature distribution. In Fig. 5, comparisons between the predicted fluid bulk temperature distributions along the channel using the simple model and numerically simulated results in the study of Qu and Mudawar [11] are shown. For the two Reynolds numbers and heat flux studied, it is seen

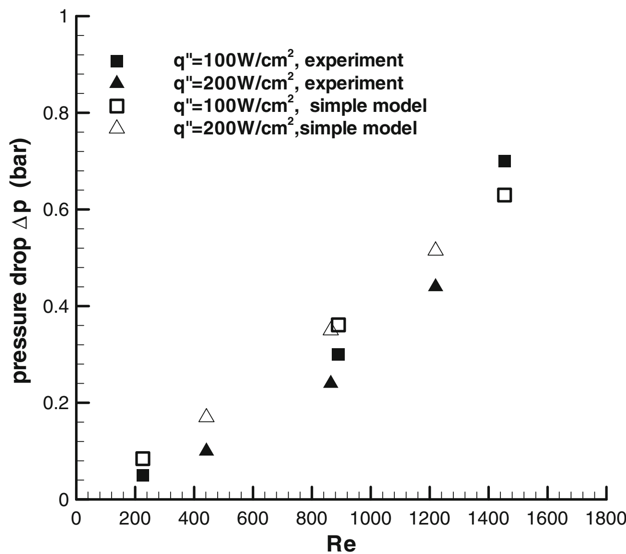

Fig. 6 Comparison of pressure drop across the micro-channel heat sink predicted by simple model with experimentally measured data by Qu and Mudawar [11]

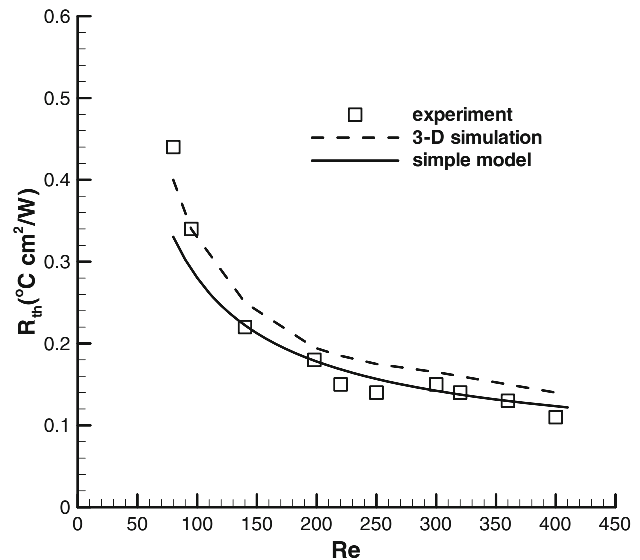

Fig. 7 Comparison of thermal resistance of microchannel heat sink predicted by simple model with experimentally measured data by Kawano et al. [25] and three-dimensional numerical simulation by Qu and Mudawar [10]

that the agreement is also good. The fluid bulk temperatures vary linearly along the channel length. Since three-dimensional computation was carried out in the study of Qu and Mudawar [11], detail temperature variation at the fluid-wall interface can be modeled. However, numerical error was involved in the three-dimensional numerical model. The simple model presented in this study is simply a one-dimension formulation in which the detail temperature variation at the fluid-wall cannot be modeled. Therefore, the discrepancy exists between the numerical results from Qu and Mudawar [11] and from the simple model is expected as shown in Fig. 5.

In Fig. 6 the pressure drop as function of the Reynolds number predicted using Eq. 20 is compared with the experimental data measured in the study by Qu and Mudawar [11]. As shown in Fig. 6, the pressure drop obtained using Eq. 21 is slightly larger than the measured data. As pointed out in the study by Li et al. [8], thermo-physical properties of the fluid can significantly influence both the flow and heat transfer in the MCHS. Since the fluid viscosity decreases with the increase of fluid temperature, this leads to an over-prediction on the pressure drop when constant viscosity is assumed. Although there exists discrepancy between predicted and measured pressure drops, the variation trend predicted by Eq. 20 agrees well with the measured data as shown in Fig. 6.

We next compared the thermal resistance of heat sink predicted using the simple model with the experimental data reported by Kawano et al. [25] and Qu and Mudawar [10]. In the study of Kawano et al. [25] and Qu and Mudawar [10], a silicon MCHS having the dimensions of $W_{ch} = 57$ μm, $H_{ch} = 180$ μm, L = 10 mm, $W_f = 43$ μm and $H_b = 270$ μm was employed. Using these dimensions, the thermal resistance of heat sink predicted by the simple model and those reported by Kawano et al. [25] and Qu and Mudawar [10] are shown in Fig. 7. As indicated in Fig. 7, the thermal resistance as function of Reynolds number predicted by the simple model is also in good agreement with the measured and three-dimensional numerical results.

3.2 Microchannel heat sink optimization using the simple model

To further verify the capability of the simple model developed in this study, the microchannel heat sink optimization using this simple model is also carried out and compared with the results available in the literature. In order to compare with the numerical simulation results reported by Li and Peterson [9], the same heat sink size and material (silicon) and optimization scheme used in their study are employed in this study. The optimization objective is to seek the microchannel geometry that results in minimum heat sink thermal resistance under the constraints of constant pumping power and fixed size of the heat sink. The microchannel heat sink has the size of $W \times H \times L = 10$ mm $\times$ 0.9 mm $\times$ 10 mm and pumping power is fixed at 0.05 W. The number of channel is determined as $N = W/(W_f + W_{ch})$. In general, N is an integer number in the practical MCHS design. For a fixed

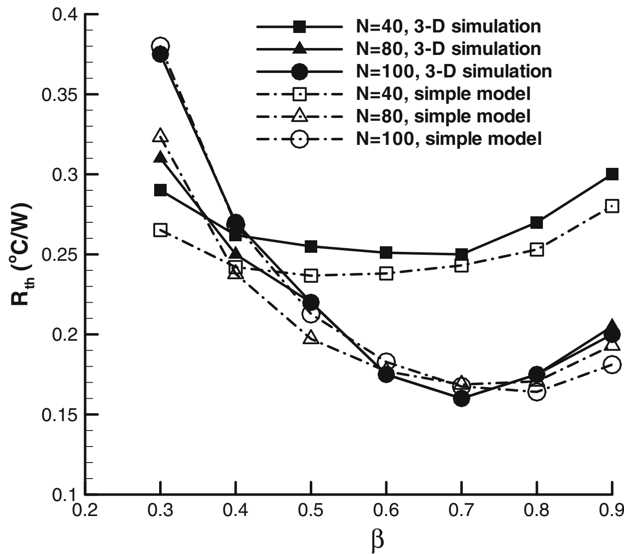

Fig. 8 Comparison of the thermal resistance of micro-channel heat sink as function of β predicted by simple model with three-dimensional simulation results of Li and Peterson [9]. H_{ch} = 360 μm

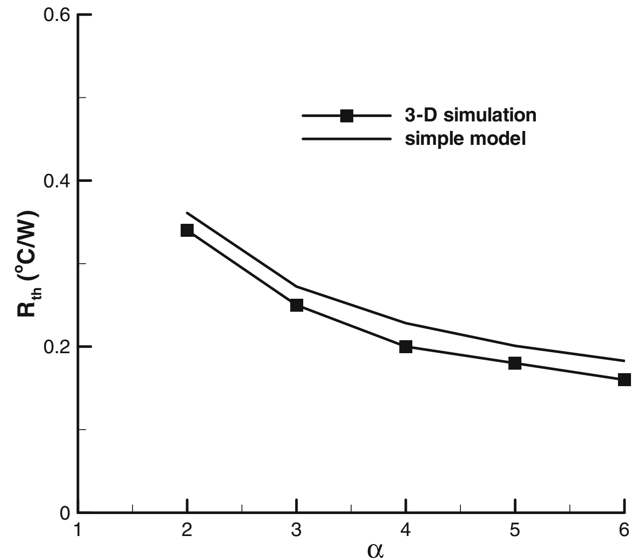

Fig. 9 Comparison of the thermal resistance of micro-channel heat sink as function α predicted by simple model with three-dimensional simulation results of Li and Peterson [9]. $N = 100$ and $\beta = 0.6$

heat sink width of W = 10 mm and requiring N to be an integer, possible channel pitches are 40, 50, 80, 100, 125, 200 and 250 μm. The corresponding numbers of channel are 250, 200, 125, 100, 80, 50 and 40, respectively. It is noted that for such channel arrangement, the thickness of end walls that forming the heat sink has been neglected.

The pumping power $\bar{P}$ required for the heat sink operation can be written as,

$$\bar{P} = \dot{V} \cdot \Delta p = N \cdot u_m \cdot W_{ch} H_{ch} \cdot \Delta p \tag{24}$$

where $\dot{V}$ is the total volume flow rate. As shown in Eq. 24, the mean velocity in the channel is related to the channel dimensions under a constant pumping power. That is, any variation in W_{ch}, H_{ch} or W_f results in different mean velocity, pressure drop and thermal resistance. As pointed out in the study by Li and Peterson [9], the ratio of the channel width to channel pitch β $(=W_{ch}/(W_f + W_{ch}))$ and the channel aspect ratio α are the two parameters used in carrying out the geometric micro-channel optimization with a fixed pumping power. In Fig. 8, we first compare the predicted thermal resistance as function of β for various numbers of channel with those reported by Li and Peterson [9] for the channel height of H_{ch} = 360 μm. Note that the comparisons are only made for the cases of N = 40, 80 and 100 since the other channel numbers used in the study by Li and Peterson [9] are not practically reachable. As shown in Fig. 8, it is seen that the agreement between the predicted and simulated results is quite well. The optimum β value that produces the lowest thermal resistance occurs in the range of 0.6–0.8 for the channel numbers studied. The effects of α on the thermal resistance with $N = 100$, $\beta = 0.6$ and $\bar{P} = 0.05\,\mathrm{W}$ are shown in Fig. 9 for both predicted from the simple model and those of Li and Peterson [9]. The agreements between these two studies are also in good agreement. As expected, the thermal resistance reduces as the channel aspect ratio increases for a fixed value of β.

The important parameters or values for optimal channel geometry analysis obtained using the simple models and those reported in the study by Li and Peterson [9] are summarized and compared in Table 2. Once again, the comparisons are made for only the cases with N = 40, 80, and 100. The error percentage of the results predicted from the simple model relative to the numerical solutions of Li and Peterson [9] are also shown in Table 2. As shown in Table 2, the agreements in pressure drop, mean velocity, Reynolds numbers and thermal resistance are quite well. In general, the relative error is within 5% for the each parameter listed in Table 2. In the N = 40 case, the Reynolds number and pressure drop have the larger errors among the cases studied. Since the thermal entrance length is proportional to the Reynolds number, it is expected that large portion of the microchannel length is in the thermal developing region. For such case, the simple model which neglecting the transverse velocity may not be accurate in predicting the actual fluid flow in the microchannel.

Table 2 Comparisons of important parameters and values on the microchannel heat sink optimization between the simple model and three-dimensional numerical simulation

H_{ch} (μm)	N	β	D_h (μm)	Δp (kPa) Numerical [9]/simple model (error %)	u_m (m/s) Numerical [9]/simple model (error %)	Re Numerical [9]/simple model (error %)	R_{th} (°C/W) Numerical [9]/simple model (error %)
360	40	0.7	235	11.98/12.6 (4.92)	2.01/2.02 (0.498)	544/557 (2.39)	0.251/0.243 (3.19)
	80	0.7	141	17.75/18.4 (3.66)	1.12/1.125 (0.446)	180/184 (2.22)	0.167/0.1687 (1.02)
	100	0.7	117	21.81/22.18 (1.69)	0.91/0.915 (0.55)	122/124 (1.64)	0.162/0.1675 (3.40)
180	80	0.7	117	27.91/29.1 (4.26)	1.42/1.43 (0.70)	192/197 (2.60)	0.252/0.258 (2.38)
	100	0.8	110	28.00/28.86 (3.07)	1.24/1.25 (0.81)	158/161 (1.90)	0.23/0.236 (2.61)

4 Conclusion

In this study, a simple model was established to predict the performance of the microchannel heat sink based on simple one-dimensional energy balance. Both the hydrodynamically and thermally developing effects on the pressure drop and heat transfer were included in this model. Based on the comparisons with the experimental data, it is found that the simple model provide satisfactory results. The simple model is further employed to carry out geometric optimization on the microchannel heat sink. The optimized results obtained from the simple model are compared with those obtained from three-dimensional simulations. Good agreement was found except when a high flow Reynolds number was involved. It is then concluded that the simple model developed in this study is adequate for employment in the heat sink design without time-consuming computations or experiments.

References

1. Kandlikar SG, Grande WJ (2003) Evolution of microchannel flow passages: thermo-hydraulic performance and fabrication technology. Heat Transf Eng 24:3–17
2. Tuckerman DB, Pease RF (1981) High-performance heat sinking for VLSI. IEEE Electron Device Lett EDL-2:126–129
3. Knight RW, Hall DJ, Goodling JS, Jaeger RC (1992) Heat sink optimization with application to microchannels. IEEE Trans Comput Hybrids Manuf Tech 15:832–842
4. Zhang HY, Pinjala D, Wong TN, Joshi YK (2005) Development of liquid cooling technologies for flip chip ball grid array packages with high heat flux dissipations. IEEE Trans Compon Packag Technol 28:127–135
5. Zhao CY, Lu TJ (2002) Analysis of micro channel heat sinks for electronics cooling. Int J Heat Mass Transf 45:4857–4869
6. Kim SJ, Kim D (1999) Forced convection in microstructures for electronic equipment cooling. ASME J Heat Transf 121:639–645
7. Fedorov AG, Viskanta R (2000) Three-dimensional conjugate heat transfer in the microchannel heat sink for electronic packaging. Int J Heat Mass Transf 43:399–415
8. Li J, Peterson GP, Cheng P (2004) Three-dimensional analysis of heat transfer in a micro-heat sink with single phase flow. Int J Heat Mass Transf 47:4215–4231
9. Li J, Peterson GP (2006) Geometric optimization of a micro heat sink with liquid flow. IEEE Trans Comput Packag Tech 29:145–154
10. Qu W, Mudawar I (2002) Analysis of three-dimensional heat transfer in micro-channel heat sinks. Int J Heat Mass Transf 45:3973–3985
11. Qu W, Mudawar I (2002) Experimental and numerical study of pressure drop and heat transfer in a single-phase micro-channel heat sink. Int J Heat Mass Transf 45:2549–2565
12. Liu S, Zhang Y, Liu P (2007) Heat transfer and pressure drop in fractal micro channel heat sink for cooling of electronic chips. Heat Mass Transf 44:221–227
13. Husain A, Kim KY (2011) Thermal transport and performance analysis of pressure- and electroosmotically-driven liquid flow microchannel heat sink with wavy wall. Heat Mass Transf 47:93–105
14. Lee P, Garimella SV, Liu D (2005) Investigation of heat transfer in rectangular microchannels. Int J Heat Mass Transf 48:1688–1704
15. Xia G, Chai L, Wang H, Zhou M, Cui Z (2011) Optimum thermal design of microchannel heat sink with triangular reentrant cavities. Appl Therm Eng 31:1208–1219
16. Lewandowski T, Ochrymiuk T, Czerwinska J (2011) Modeling of heat transfer in microchannel gas flow. ASME J Heat Transf 133:1–15
17. Raisi A, Ghasemi B, Aminossadati SM (2011) A numerical study on forced convection of laminar nanofluid in a microchannel with both slip and no-slip conditions. Numer Heat Transf A Appl 59:114–129
18. Tiselj I, Hetsroni G, Mavko B, Mosyak A, Pogrebnyak E, Segal Z (2004) Effect of axial conduction on the heat transfer in micro-channels. Int J Heat Mass Transf 47:2551–2565
19. Peng H, Ling X (2008) Experimental investigation on flow and heat transfer performance of a novel heat fin-plate radiator for electronic cooling. Heat Mass Transf 45:1575–1581

20. Hong FJ, Cheng P, Wu HY (2011) Characterization on the performance of a fractal-shaped microchannel network for microelectronic cooling. J Micromech Microeng 21:065018
21. Chen T, Garimella SV (2011) Local heat transfer distribution and effect of instabilities during flow boiling in a silicon microchannel heat sink. Int J Heat Mass Transf 54:3179–3190
22. Lee P, Garimella SV (2006) Thermally developing flow and heat transfer in rectangular microchannels of different aspect ratios. Int J Heat Mass Transf 49:3060–3067
23. Phillips RJ (1987) Microchannel heat sinks, Ph.D. thesis, Massachusetts Institute of Technology
24. Shah RK, London AL (1978) Laminar flow forced convection in ducts: a source book for compact heat exchanger analytical data, Suppl 1. Academic Press, New York
25. Kawano K, Minakami K, Iwasaki H, Ishizuka M (1998) Micro channel heat exchanger for cooling electrical equipment. Application of Heat Transfer in Equipment, Systems, and Education, ASME HTD-361-3/PID-3:173–180
26. Kandlikar SG, Garimella SV, Li D, Colin S, King MR (2006) Heat transfer and fluid flow in minichannels and microchannels. Elsevier, Singapore
27. Mills AF (1999) Heat transfer, 2nd edn. Prentice Hall, Upper Saddle River